Optimal control for load alleviation in wind turbines

Bart P.G. Van Parys[1], Bing Feng Ng[2], Paul J. Goulart[1], and Rafael Palacios[2]

[1]*Automatic Control Laboratory, Swiss Federal Institute of Technology, Zürich, CH*
[2]*Department of Aeronautics, Imperial College London, UK*

Nowadays, trailing edge flaps on wind turbine blades are considered to reduce loading stresses in wind turbine components. In this paper, an optimal control synthesis methodology for the design of gust load controllers for large wind turbine blades is proposed. We discuss a control synthesis approach that minimises the power expenditure of the actuated trailing edge flap, while at the same time guaranteeing that certain blade load measures remain bounded in a *probabilistic* sense. To illustrate our proposed control design methodology, a standard NREL 5-MW reference turbine was considered. The obtained numerical results indicate that through the use of optimal feedback considerable reductions in loading stresses could be achieved for moderate actuation power.

Nomenclature

Wind turbine:
ν Position and orientation of wind turbine hub with respect to the ground
η Positions and orientations of wind turbine blades with respect to the hub
M_x Root torsion moment $[N \cdot m]$
M_y Root bending moment $[N \cdot m]$
r_x Blade tip rotation $[rad]$
q_z Blade tip displacement $[m]$
β Flap actuation angle $[rad]$

Wind flow:
$\nabla\Phi$ Air flow speed around blade $[m/s]$
n_{gust} Wind gust speed $[m/s]$
τ Atmospheric turbulence level $[\%]$

Optimal control:
J Cost function
$\boldsymbol{K}$ Control policy
ϵ Constraint satisfaction level

I.   Introduction

THE size of wind turbines has been increasing steadily over the years, and rotors measuring up to 160 meter in diameter are being developed [1]. However, unfavourable aeroelastic behaviour as a result of increased length and flexibility of the blades can raise blade safety concerns and increase structural degradation [2]. A cost-efficient alternative to a large increase in stiffness is the use of stronger materials and localised active control techniques to overcome extreme blade loading and excessive oscillations.

Pitch actuation methods, which already exist on wind turbines for speed regulation and have been shown to be effective in load alleviation, are only able to suppress lower frequency loading [3]. To overcome such limitations, distributed load alleviation actuators placed along different sections of the blades can be designed to complement existing pitch control mechanisms by addressing the higher frequency loadings. For instance, using trailing-edge flaps for load reduction, Frederick *et al.* [4], Riziotis *et al.* [5] and Basualdo [6] were able to achieve significant reduction in blade loading and aerofoil displacements, while Barlas *et al.* [7, 8] and

American Institute of Aeronautics and Astronautics

Wilson *et al.* [9], demonstrated the performance benefits of multiple flaps on a full rotor.

In this paper, we discuss a control synthesis approach that minimises the power expenditure of the actuated trailing edge flap, while at the same time guarantees that certain blade load measures remain bounded. In particular, we use the distributionally robust control approach discussed in Van Parys *et al.* [10] to synthesise control policies that guarantee that the root bending moments and tip deflections experienced by the blades remain small in a probabilistic sense. The distributionally robust control approach can be interpreted as constrained linear quadratic control, since the former approach reduces to standard linear-quadratic-Gaussian (LQG) control in the absence of the blade load constraints.

Past work in blade load control has relied heavily on classical control methods, such as PD and PID control [4]. Since the focus of initial work was on developing proofs-of-concept, more advanced control techniques were not investigated. More recent work has considered optimal control synthesis approaches such as $\mathcal{H}_2$ or $\mathcal{H}_\infty$ optimal control [4, 11, 12] and model predictive control (MPC) methods [8, 13]. However, in these more recent works the cost functions employed did not reflect any particular control design objective, but rather were treated as tuning parameters with which to synthesise controllers that met the blade load requirements *ex post facto*. The main advantage of the approach taken in this paper over the existing synthesis techniques is that they guarantee bounded blade load measures by construction, and hence only require minor tuning. As our synthesis approach yields explicit linear controllers, they also represent less of a computational burden than standard MPC implementations.

Outline : In Section II, the structural and aerodynamic model of the wind turbine used in this paper is briefly described. Section III introduces the distributionally robust framework. Additionally, the approach can be seen as a natural generalisation of standard LQG control with a relaxation of the standard atmospheric turbulence assumption. The performance of the synthesised optimal controller for a benchmark turbine developed by the National Renewable Energy Laboratory (NREL) [8, 14, 15] is discussed in Section IV.

Notation and definitions

We denote by $\mathbb{I}_n$ the identity matrix in $\mathbb{R}^{n \times n}$ and by $\mathbb{S}^n_+$ and $\mathbb{S}^n_{++}$ the sets of all positive semi-definite and positive definite symmetric matrices in $\mathbb{R}^{n \times n}$, respectively. A signal is a measurable function that maps the natural numbers $\mathbb{N}$ to $\mathbb{R}^n$. A system is a mapping from the input signal space $\mathcal{S}_1$ to the output signal space $\mathcal{S}_2$, i.e. $\boldsymbol{G} : \mathcal{S}_1 \to \mathcal{S}_2$, and will be denoted in upper-case bold. We assume throughout that all systems are linear, i.e. $\boldsymbol{G}(n_1 + n_2) = \boldsymbol{G}n_1 + \boldsymbol{G}n_2$, $\forall n_1, n_2 \in \mathcal{S}_1$. A small bold letter $\boldsymbol{w}$ indicates a stochastic process $\boldsymbol{w} : \Omega \to \mathcal{S}$ defined on the abstract probability space $(\Omega, \mathcal{F}, \mathbb{P}^\star)$, where Ω is referred to as the sample space, $\mathcal{F}$ represents the σ-algebra of events and $\mathbb{P}^\star$ denotes a probability measure. The set $\mathcal{P}_0$ contains all probability measures on $(\Omega, \mathcal{F})$, i.e. we have $\mathbb{P}^\star \in \mathcal{P}_0$. The function $\delta : \mathbb{R} \to \mathbb{R}$ is defined as $\delta(0) = 1$ and zero otherwise.

II.   Aeroservoelastic Model

Throughout, we use the standard NREL 5-MW reference wind turbine [16] to illustrate our control design methods. This wind turbine was developed to support conceptual studies aimed at accessing offshore wind technology and has been widely adopted as a benchmark case for the aeroelastic analysis and design of large flexible wind turbines [8, 14, 15].

The aeroservoelastic model of the wind turbine presented here has been developed according to the Simulation of High Aspect Ratio Planes (SHARP) [17–20] framework. The SHARP framework has been extensively verified in flexible aircraft applications. Moreover, in recent work [21] it was tailored to model the dynamics of large wind turbine blades. In the SHARP framework, a non-linear composite beam model is coupled together with the Unsteady Vortex Lattice Method (UVLM) describing the airflow around the wing blades. In subsequent sections, a brief overview of both structural and aerodynamic models coupled according to Figure 1 will be presented.

II.A.   Composite beam model of the wind turbine blades

The blades have been reduced to one dimensional beams using a variational asymptotic cross-sectional analysis [22] able to cope with large static and dynamic deformations, as illustrated in Figure 2. The structural model describes the displacements and rotations of this composite beam structure [23, 24] under the influence of localised nodal external forces Q_{ext}. For the purpose of efficient control synthesis, the non-linear model was linearised around a steady-state operating condition. In what follows, attention is limited

American Institute of Aeronautics and Astronautics

Nodal displacement orientations,
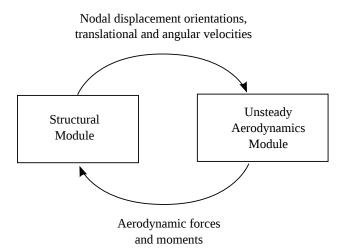translational and angular velocities

Figure 1. Coupling between structural and aerodynamic modules in SHARP.
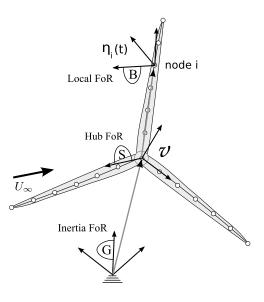
to a single blade.

Figure 2. Multi-beam configuration of the wind turbine with the definition of reference frames for the structural model.

As shown in Figure 2, the motion of the blade is described in a hub-fixed reference coordinate system S, which moves with rotational velocities $v_G(t) \in \mathbb{R}^3$ and $\omega_G(t) \in \mathbb{R}^3$ in the inertial reference frame G. The displacements $v_S^i(t) \in \mathbb{R}^3$ and rotations $\omega_S^i(t) \in \mathbb{R}^3$ of node $i \in [1, \ldots, p]$ along the beam are described with respect to the hub fixed reference frame S. The equations of motion for the structural dynamics system are partially given by the second order ordinary differential equation (ODE) [18, 24] in (η, ν)

$$\mathcal{M}_\eta(\eta)\,\ddot{\eta} + m_\nu(\eta, \dot{\eta})\,\dot{\nu} + Q_{gyr}(\eta, \nu) + Q_{stif}(\eta) = Q_{ext}, \tag{1}$$

where the vector $\eta(t) = [v_S^1; \omega_S^1; \ldots; v_S^p; \omega_S^p](t) \in \mathbb{R}^{6p}$ contains all the nodal displacements and rotations describing the deformation of the beam in the reference frame S and $\nu(t) = [v_G(t); \omega_G(t)] \in \mathbb{R}^6$ describes the velocity of the hub itself with respect to the inertial reference frame G. The generalised mass matrix $\mathcal{M}_\eta(\eta) \in \mathbb{R}^{6p \times 6p}$, gyroscopic $Q_{gyr}(\eta, \nu) \in \mathbb{R}^{6p}$ and elastic forces $Q_{stif}(\eta) \in \mathbb{R}^{6p}$ are assumed known. The ODE (1) describes the deformations of the blade by balancing the localised internal inertial and elastic forces with the external forces $Q_{ext}(t) \in \mathbb{R}^{6p}$. The effects due to the motion $\nu(t)$ of the hub in the inertial reference frame G are incorporated through the coupling mass matrix $m_\nu(\eta, \dot{\eta}) \in \mathbb{R}^{6p \times 6}$ and the gyroscopic forces $Q_{gyr}(\eta, \nu)$.

The structural dynamic model is linearised around the steady-state operating condition $[\eta, \dot{\eta}, \nu, \dot{\nu}](t) = (0, 0, 0, \nu_0) + [\Delta\eta, \Delta\dot{\eta}, \Delta\nu, \Delta\dot{\nu}](t)$ and $Q_{ext}(t) = Q_0 + \Delta Q_{ext}(t)$. The linearised form of the beam deformation

American Institute of Aeronautics and Astronautics

model (1) is:

$$M\Delta\ddot{\eta} + m_\nu(\nu_0)\Delta\dot{\nu} + C_{gyr}\left(\nu_0\right)\Delta\nu + \left[K_{gyr}\left(\nu_0\right) + K_{stif}\right]\Delta\eta = \Delta Q_{ext}, \qquad (2)$$

where the mass matrix $M \in \mathbb{R}^{6p \times 6p}$, damping matrix $C_{gyr}(\nu_0) \in \mathbb{R}^{6p \times 6}$, stiffness matrices $K_{gyr}(\nu_0) \in \mathbb{R}^{6p \times 6p}$ and $K_{stif} \in \mathbb{R}^{6p \times 6p}$ have been obtained through direct linearisation of the different generalised forces. A more detailed derivation of the linearisation can be found in Hesse *et al.* [17]. The resulting continuous time linear system (2) was discretised using the Newmark-β method [25] for integration at a frequency of $f_s = 200$ Hz.

II.B.   Unsteady aerodynamics model

In this section, we describe briefly the forces experienced by the blades caused by the fluid flow around them under the influence of the blade movement, flap actuation and atmospheric turbulence. The airflow around the blades is modelled using the discrete-time UVLM [20, 26] with a prescribed helicoidal wake. The UVLM assumes low-speed, high Reynolds number, attached flow conditions to hold.
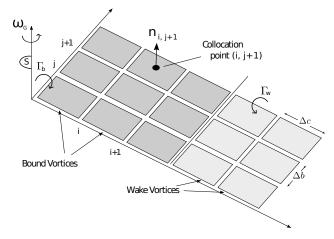

Figure 3. Typical thin lifting surface represented by the Unsteady Vortex Lattice Method.

Under the aforementioned conditions, the unsteady potential flow $\nabla\Phi(x, k) \in \mathbb{R}^3$ at position $x \in \mathbb{R}^3$ and time $k \in \mathbb{N}$ is assumed to solve the Laplace equation in the space coordinates for all times k; see Katz *et al* [26]. By merit of the superposition principle, an approximate solution satisfying Laplace's equation can be found as the linear combination

$$\Phi(x, k) = \sum\nolimits_{i,j} \Gamma_{i,j}(k)\Phi_{hom}(x - s_{i,j}),$$

where $\Phi_{hom}(x - s)$ are fundamental solutions of the Laplace equation at all locations $s \in \mathbb{R}^3$. The time dependent weights $\Gamma_{i,j}(k) \in \mathbb{R}$ are determined uniquely by enforcing boundary conditions on the flow potential Φ at fixed collocation points. The effects of flap actuation, blade movement and atmospheric turbulence are included through the particular enforced boundary conditions.

The UVLM considered here uses vortex rings [26] as fundamental solutions, which are located in lattice panels that represent the blades and their wakes. The leading segment of the vortex ring is placed along the quarter chord of each panel. The geometry of this model is sketched in Figure 3.

To determine the potential flow $\nabla\Phi$, Neumann boundary conditions [26] are enforced at the three-quarter chord of each panel, thereby fulfilling the Kutta-Joukowski condition. Hence, the normal velocity at each collocation point due to the potential flow and motion of the blade must be zero, i.e. there is no flow passing through the blades. The Neumann boundary conditions in vectorized form are

$$A_c\Gamma(k) + w(k) = 0,$$

where $\Gamma(k) \in \mathbb{R}^q$ is a vector containing the vortex strengths $\Gamma_{i,j}(k)$ and q the total number of panels covering both the blade and wake model. The columns of the matrix $A_c \in \mathbb{R}^{q \times q}$ contain the induced normal velocity to the blade surface at the collocation points due to the corresponding *vortex ring* flow $\nabla\Phi_{hom}(x - s_{i,j})$.

American Institute of Aeronautics and Astronautics

The term $w(k) \in \mathbb{R}^q$ is the downwash at the collocation points and is caused by the motion of the blade $w_{blade}(k) \in \mathbb{R}^q$, the trailing-edge flap $w_{flap}(k) \in \mathbb{R}^q$, and atmospheric turbulence $w_{gust}(k) \in \mathbb{R}^q$, such that

$$w(k) = w_{blade}(k) + w_{flap}(k) + w_{gust}(k). \tag{3}$$

The terms (w_{blade}, w_{flap}) and w_{gust} are treated as the endogenous and exogenous input to the aerodynamic model, respectively. The output of the model are the forces $F_{i,j}(k) \in \mathbb{R}^3$ caused by the fluid flow experienced by the blade at all collocation points. These forces

$$F_{i,j}(k) = [\Delta p_{i,j}(k)\Delta c\Delta b] \cdot n_{i,j} \tag{4}$$

are related to the pressure differences $\Delta p_{i,j}(k) \in \mathbb{R}$ across each panel on the lifting surface determined using the *linear* unsteady Bernoulli equation [19]. The normal vectors $n_{i,j} \in \mathbb{R}^3$ of the blade panels are considered to be known and fixed in the reference frame S.

II.C.   The overall system

The discretised structural equations of motion (2) are coupled with the discrete-time UVLM as illustrated in Figure 1. As the lifting surface is comprised of panels in a lattice, while the beam structure is composed of nodes along a curve, the aerodynamic forces $F_{i,j}$ determined in equation (4) are approximated by a linear interpolation mapping of the external force Q_{ext} in Equation (2). In turn, the nodal orientations, translational and angular velocities represented by η and $\dot{\eta}$ are mapped linearly onto the collocation points as downwash w_{blade} in Equation (3).

Moreover, we have at our disposal a linear time-invariant (LTI) gust system that determines the input $w_{gust}(k)$ in case of an incoming transversal gust with strength $n_{gust}(k) \in \mathbb{R}$. Similarly, we have an LTI system determining the input $w_{flap}(k)$ where we assume the flap to be torque controlled with torque input $u(k) \in \mathbb{R}$. The gust and flap model and the mappings discussed in the last paragraph are omitted for the sake of brevity, but the overall blade model $\boldsymbol{T}$ is illustrated as a block diagram in Figure 4.
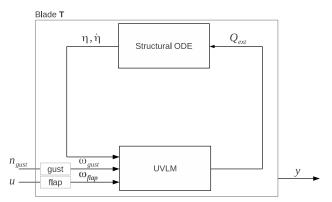

Figure 4. The overall system T is a combination of the structural model introduced in Section II.A and the aerodynamic model of Section II.B. The grey boxes denote LTI systems omitted for the sake of brevity.

In the next section, we will be interested in constructing a control policy which minimises the expected actuation power consumption while keeping several blade load measures within specified bounds. The considered control policies are restricted to be causal functions of the measured outputs $y(k) \in \mathbb{R}^3$ which consist of the torsion M_x, the root bending moment M_y and the out-of-plane tip deflection q_z as illustrated in Figure 6.

III.   Constrained LQG control

The purpose of feedback control for load alleviation in wind turbines is to minimise actuation expenditure, while keeping several measures of blade loading within specified bounds. As is common in control applications, atmospheric turbulence is treated in this paper as a stochastic stationary process with known power spectrum. This stochastic turbulence model places our control problem in a distributionally robust optimal control framework [10], closely related to the standard $\mathcal{H}_2$ or LQG control [27] framework.

American Institute of Aeronautics and Astronautics

When the control objective is a quadratic function of the inputs and outputs of the system, it is well known that the optimal controller in the $\mathcal{H}_2$ sense is the LQG controller. However, we wish to take into account several additional blade load constraints, which requires us to employ a more sophisticated distributionally robust optimal control method.

Distributionally robust control can be interpreted as constrained linear quadratic control, since the former approach reduces to standard LQG control in the absence of constraints. This more advanced framework allows us additionally to relax the standard atmospheric turbulence assumptions [28], as will be discussed in the next section.

III.A. The nature of atmospheric turbulence

In control applications, atmospheric turbulence is most commonly treated as a stochastic disturbance with a standardised spectrum, e.g. a von Kármán or Kaimal spectrum [28]. This standardised power spectrum is then encoded in a LTI filter chosen to generate an output with the appropriate turbulence spectrum when driven by a white noise input, as shown in Figure 5. It is assumed here that the standard turbulence spectrum is not affected by the movement of wind turbine blades. A classical result of Kolmogorov [29]
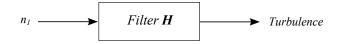
$$n_1 \longrightarrow \boxed{\textit{Filter } \boldsymbol{H}} \longrightarrow \textit{Turbulence}$$

Figure 5. The von Kármán turbulence model.

argues that the spectrum of turbulence decays in the high frequency limit as $s^{-5/3}$, having as a consequence that no filter with a turbulence spectrum admits a finite order state space representation. The third order turbulence filter presented in [30] can be used as a finite order approximation.

The preference for Gaussian noise in most of the control and economic literature as a stochastic model for the disturbance input is based on both theoretical and practical observations. Theoretically, the response $\boldsymbol{x}(k)$ of LTI systems to a Gaussian process $\boldsymbol{n}$ is well characterised, i.e. the distribution of the response $\boldsymbol{x}(k)$ remains Gaussian for all times k if $\boldsymbol{x}(0)$ is Gaussian as well. Practically, the Gaussian assumption avoids the problem of having to specify a probability measure $\mathbb{P}^\star$ for the disturbance process $\boldsymbol{n}$, as the Gaussian process is fully determined by only its mean and covariance function.

It is clear that atmospheric turbulence is unlikely to be Gaussian in practice. Hence, we consider a more general disturbance model. However, we would like to retain both the theoretical and practical advantages of working with a Gaussian process. That is, we want only to specify a mean and covariance function and to have a property mirroring the invariance property of Gaussian processes for linear systems. In the following, we therefore assume that $\boldsymbol{n}$ is a white zero-mean weak-sense stationary (w.s.s.) stochastic process with probability measure

$$\mathbb{P}^\star \in \mathcal{P} := \left\{ \mathbb{P} \in \mathcal{P}_0 \ \big| \ \mathbb{E}_\mathbb{P}\left\{\boldsymbol{n}(k)\right\} = 0, \ \mathbb{E}_\mathbb{P}\left\{\boldsymbol{n}(k_1) \cdot \boldsymbol{n}(k_2)^\top\right\} = R_n(k_1, k_2) = \mathbb{I}_d \delta(k_1 - k_2) \right\}.$$

The true but unknown probability measure $\mathbb{P}^\star$ is hence not necessarily Gaussian, and is only known to belong to the *distributional ambiguity* set $\mathcal{P}$. It should be clear that the distributional ambiguity set $\mathcal{P}$ depends only on the covariance function $R_n(k_1, k_2)$. We have additionally an invariance property for w.s.s. processes mirroring the invariance property for Gaussian processes, i.e. the response of a linear system to a w.s.s. process is a w.s.s. process itself [31].

It can be shown, by applying the Wiener-Khinchine Theorem, that $\mathcal{P}$ is the biggest set such that the turbulence $\boldsymbol{n}_{gust} = \boldsymbol{H}\boldsymbol{n}_1$ has a von Kármán spectrum. Hence, our turbulence model is not a uniquely defined random process, but the biggest set of random processes sharing the von Kármán spectrum as was originally envisioned by Kolmogorov [29].

III.B. Control design objectives

The distributionally robust optimal controller [10] minimises a quadratic cost function, similar as the LQG controller. In the context of load alleviation, a natural cost function is the square of the expected flap actuation power consumption, defined as

American Institute of Aeronautics and Astronautics

$$J := \overline{\lim}_{N\to\infty} \sup_{\mathbb{P}\in\mathcal{P}} \frac{1}{N}\mathbb{E}_{\mathbb{P}}\left\{\sum_{k=0}^{N-1}\ddot{\boldsymbol{\beta}}^2(k)\right\}. \tag{5}$$

where $\boldsymbol{\beta}(t)$ is the flap actuation angle. However, this cost function has no regard for blade loading or any other physical consideration as it only measures actuation power consumption. Indeed, the unconstrained optimal LQG controller that minimises the cost J reduces in this case to no control at all. Hence, in what follows we will only consider control policies that ensure that the closed-loop system satisfies additional probabilistic blade load constraints. In the light of these restrictions, the proposed distributionally robust control method can be considered a constrained LQG method.
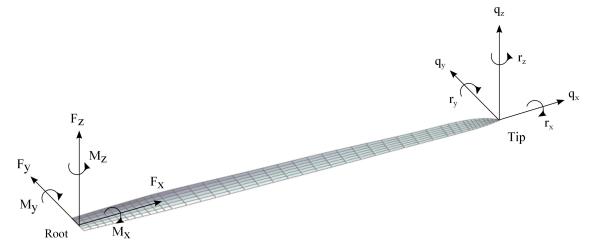

Figure 6. Description of forces/moments and tip displacements/rotations on the blade.

BLADE LOAD CONSTRAINTS :   The primary reason for our introduction of a trailing-edge flap is the reduction of blade load stresses using feedback control. We will reduce the blade load severity to two key blade load indicators; the root-bending moment (RBM) $\boldsymbol{M}_y$ and out-of-plane tip deflection $\boldsymbol{q}_z$, as shown in Figure 6. Both the RBM and tip deflection are key load indicators, since the root of the blade is a critical area supporting the blade and is constantly subjected to large cyclic and fluctuating loads, while tip deflection determines among other things whether the blade is in risk of contact with the tower. In the distributionally robust setting, these considerations are translated into the constraints

$$\forall k \in \mathbb{N}, \ \forall \mathbb{P} \in \mathcal{P}: \quad \begin{cases} \mathbb{P}\{-M_y^n \leq \boldsymbol{M}_y(k) \leq M_y^n\} \geq 1-\epsilon \\ \mathbb{P}\{-q_z^n \leq \boldsymbol{q}_z(k) \leq q_z^n\} \geq 1-\epsilon \end{cases} \tag{6}$$

for the closed loop system. Informally, the last requirements read that both the RBM and tip deflection are less in absolute value than their nominal limits M_y^n and q_z^n, respectively, with a probability of at least $1-\epsilon$ for all times k. The active flap actuation is expected to yield additional blade torsion loads. We require the torsion $\boldsymbol{M}_x$ in the blade to be bounded as

$$\forall k \in \mathbb{N}, \ \forall \mathbb{P} \in \mathcal{P}: \quad \mathbb{P}\{-M_x^n \leq \boldsymbol{M}_x(k) \leq M_x^n\} \geq 1-\epsilon. \tag{7}$$

ADDITIONAL PHYSICAL CONSTRAINTS :   In addition to the blade loading constraints, constraints on the flap actuation angle and angle of attack (AOA) of the blades are also required. To ensure physical realizability, the flap actuation angle should be bounded [16]. Hence, we require the following constraint to hold

$$\forall k \in \mathbb{N}, \ \forall \mathbb{P} \in \mathcal{P}: \quad \mathbb{P}\{-\beta^n \leq \boldsymbol{\beta}(k) \leq \beta^n\} \geq 1-\epsilon. \tag{8}$$

The UVLM model in the aeroelastic formulation operates under an incompressible flow assumption in which viscous effects are neglected. Moreover, the lifting surfaces are assumed to be thin and the AOA of the blade is assumed to remain small. Hence to ensure the validity of the model and smooth operation of the wind

turbine, the magnitude of the blade's AOA and its change over time are required to be sufficiently small, thereby avoiding both dynamic and static flow separations. We model these requirements as

$$\forall k \in \mathbb{N}, \ \forall \mathbb{P} \in \mathcal{P} : \quad \begin{cases} \mathbb{P}\{-r_x^n \leq \boldsymbol{r}_x(k) \leq r_x^n\} \geq 1 - \epsilon \\ \mathbb{P}\{||\dot{\boldsymbol{r}}_x(k)/\dot{r}_x^n, \dot{\boldsymbol{q}}_z(k)/\dot{q}_z^n||_2 \leq 1\} \geq 1 - \epsilon \end{cases} \tag{9}$$

Observe that all of our design constraints are required to hold for all $\mathbb{P} \in \mathcal{P}$ and not merely for the case that $\boldsymbol{n}$ happens to be a Gaussian process. This explains the use of the term *distributionally robust* when characterising this approach.

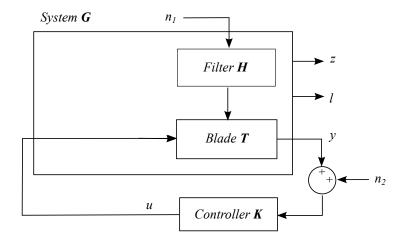**Figure 7. Visualisation of the control set-up. A controller $\boldsymbol{K} : y \mapsto u$ needs to be found that minimises the cost output z, while keeping the load output ℓ bounded. The overall system $\boldsymbol{G}$ consists of the blade model $\boldsymbol{T}$ and von Kármán filter $\boldsymbol{H}$.**

The different LTI systems introduced throughout this paper so far can be combined to define an overall model $\boldsymbol{G}$, as shown in Figure 7. To simplify the exposition in subsequent sections, we make the following standard assumptions. We assume that the system model $\boldsymbol{G}$ admits the following state space representation

$$\begin{aligned} x(k+1) &= Ax(k) + Bu(k) + Cn(k) \quad \text{and} \quad x(0) = 0 \\ y(k) &= Dx(k) + En(k), \end{aligned} \tag{$\boldsymbol{G}$}$$

with $EC^\top = 0$ and where the zero initial condition reflexes the fact that the transient response $DA^k x(0)$ of the system is not of interest. The system matrices have the dimensions $A \in \mathbb{R}^{a \times a}$, $B \in \mathbb{R}^{a \times b}$, $C \in \mathbb{R}^{a \times d}$, $D \in \mathbb{R}^{r \times a}$ and $E \in \mathbb{R}^{r \times b}$. Moreover, without further loss of generality we assume there exists matrices $E_i \in \mathbb{R}^{p_i \times n}$, $i \in [1, \ldots, 6]$ such that the constraints (6)-(9) reduce to

$$\forall k \in \mathbb{N}, \ \forall \mathbb{P} \in \mathcal{P} : \quad \mathbb{P}\{||\boldsymbol{\ell}_i(k)||_2 \leq 1\} \geq 1 - \epsilon,$$

with $\ell_i(k) = E_i x(k)$. Similarly for the cost function (5), we assume there exists matrices $Q \in \mathbb{S}_+$, $R \in \mathbb{S}_{++}$ such that

$$J = \overline{\lim}_{N \to \infty} \quad \sup_{\mathbb{P} \in \mathcal{P}} \ \frac{1}{N} \mathbb{E}_\mathbb{P} \left\{ \sum_{k=0}^{N-1} \boldsymbol{z}(k)^2 \right\} = \overline{\lim}_{k \to \infty} \quad \sup_{\mathbb{P} \in \mathcal{P}} \ \mathbb{E}_\mathbb{P} \left\{ \boldsymbol{z}(k)^2 \right\},$$

where the second equality in last equation is shown by Kwakernaak [32] and with $z := \left(Q^{1/2}x; R^{1/2}u \right)$. The control problem for the system $\boldsymbol{G}$ with augmented outputs $\ell := (\ell_1, \ldots, \ell_6)$ and z is illustrated in Figure 7.

III.C. Distributionally robust control

We are interested in finding a control policy that minimises the actuation power consumption, while satisfying the constraints discussed in the last section. More formally, we consider the following optimal control

American Institute of Aeronautics and Astronautics

problem:

$$\inf_{\boldsymbol{K}} \quad J = \overline{\lim}_{k \to \infty} \quad \sup_{\mathbb{P} \in \mathcal{P}} \ \mathbb{E}_{\mathbb{P}} \left\{ \boldsymbol{z}(k)^2 \right\}$$
$$\text{s.t.} \quad (\boldsymbol{z}, \boldsymbol{\ell}, \boldsymbol{y}) = \boldsymbol{G}(\boldsymbol{u}, \boldsymbol{n}), \ \boldsymbol{u} = \boldsymbol{K}(\boldsymbol{y}), \tag{$\mathcal{R}_2$}$$
$$k \in \mathbb{N}, \ \forall \mathbb{P} \in \mathcal{P} : \ \mathbb{P} \left\{ \| \boldsymbol{\ell}_i(k) \|_2 \le 1 \right\} \ge 1 - \epsilon, \ \text{for all } i$$

As can be seen from Theorem III.1, the optimal causal linear control policy $\boldsymbol{K}^\star$ separates into a Kalman estimator and a certainty equivalent control gain. A similar separation between estimator and controller can be seen in the MPC approaches reported in [8,13], where this structure was however assumed *ad hoc*.

Theorem III.1 (Distributionally robust optimal control [10])**.** *The optimal linear feedback law $\boldsymbol{K}^\star : y \mapsto u$ of problem $\mathcal{R}_2$ consists of a linear estimator-controller pair (S, K) and is of the form*

$$\begin{cases} \hat{x}(k+1) = A\hat{x}_k + Bu_k + S\left(y_{k+1} - C\left(A\hat{x}_k + Bu_k\right)\right) & and \quad \hat{x}(0) = 0 \\ u(t) = K\hat{x}(k), \end{cases} \tag{$\boldsymbol{K}^\star$}$$

with $S := YD^\top \left(DYD^\top + EE^\top\right)^{-1}$. The matrix $Y \in \mathbb{S}_+^a$ is the unique positive definite solution of the discrete algebraic Riccati equation

$$Y = A\left(Y - YD^\top \left(DYD^\top + EE^\top\right)^{-1} DY\right) A^\top + CC^\top,$$

which can be solved efficiently. The static feedback matrix $K = Z^\star (P^\star)^{-1}$, where $P^\star \in \mathbb{S}_{++}^a$ and $Z^\star \in \mathbb{R}^{b \times a}$ can be found as the optimal argument of

$$\min \quad \operatorname{Tr} Q\left(\Sigma + P\right) + \operatorname{Tr} RX$$
$$\text{s.t.} \quad P \in \mathbb{S}_+^a, \ Z \in \mathbb{R}^{b \times a}, X \in \mathbb{S}_+^b$$
$$\left(\begin{smallmatrix} X & Z \\ Z^\top & P \end{smallmatrix}\right) \succeq 0, \ \operatorname{Tr}\left\{E_i\left(\Sigma + P\right)E_i^\top\right\} \le \epsilon \tag{10}$$
$$\left(\begin{smallmatrix} P - APA^\top - BZA^\top - AZ^\top B^\top - \tilde{W} & BZ \\ Z^\top B^\top & P \end{smallmatrix}\right) \succeq 0$$

where $\tilde{W} := YD^\top \left(DYD^\top + EE^\top\right)^{-1} DY^\top$ and $\Sigma = Y - \tilde{W}$.

The optimisation problem (10) is a semi-definite program (SDP) in the variables P, Z and X. This type of optimisation problem is well studied [33] and extremely efficient numerical solvers exist [34]. In fact, finding the optimal controller $\boldsymbol{K}^\star$ is computationally comparable to synthesising a standard LQG controller.
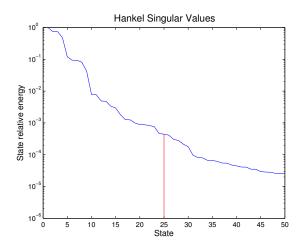
IV.   Control synthesis and performance

Using the SHARP framework briefly described in Section II, we derive a linear model of the standard NREL 5-MW reference wind turbine [16] around the stationary operating condition $\nu_0 = (v_G; \omega_G)$ with $v_G = (0; 0; 0)$ [m/s] and $\omega_G = (0; 0; 1.3)$ [rad/s]. In Table 1, we summarise the key characteristics of the resulting model $\boldsymbol{G}$. All computations were carried out in `MATLAB` with the help of the numerical optimisation solver `SDPT3` [34] used to solve problem (10).

The procedure described in Theorem III.1 can be used to construct an optimal controller $\boldsymbol{K}^\star$ for problem $\mathcal{R}_2$. The resulting controller $\boldsymbol{K}^\star$ has an order equal to the number of states in the model $\boldsymbol{G}$. However, as our system $\boldsymbol{G}$ is of considerable size, the construction of a Kalman estimator for $\boldsymbol{G}$ is already computationally challenging. Hence, in the sequel we abstain from synthesising a control policy directly from the system $\boldsymbol{G}$. Instead, we first derive a reduced system using model reduction by balanced truncation [35]. The resulting reduced system $\boldsymbol{G}_r$ has an order of 25 states, see Figure 8. As the relative size of the cut-off singular value is small, the reduced system $\boldsymbol{G}_r$ is close to the turbine model $\boldsymbol{G}$, see for instance [35]. Although the constructed control policies $\boldsymbol{K}^\star$ will be optimal only for the reduced system $\boldsymbol{G}_r$, it will be the closed loop behaviour of $\boldsymbol{G}$ and $\boldsymbol{K}^\star$ that will be investigated further; see Figure 7.

As the starting point of the analysis, we report the root mean square (RMS) norms of the considered blade root measures discussed in Section III when the system $\boldsymbol{G}$ is left uncontrolled in Table 2. The RMS norm of an output $F\boldsymbol{x}(t) \in \mathbb{R}$ is the positive root of $FPF^\top \in \mathbb{R}_+$ where $P \in \mathbb{S}_+^a$ solves the Lyapunov equation

$$APA^\top - P + C\tau^2 C^\top = 0,$$

Figure 8. The Hankel singular values of G relative to the biggest Hankel singular value are shown in the figure. The reduced system G_r is indicated with a red line.

Table 1. The most important features of the turbine model G.

Sampling frequency	$f_s = 200$ Hz
Internal states	$a = 1131$
Endogenous inputs	$\ddot{\beta}$
Exogenous inputs	n_1
Measured outputs	$\{M_x, M_y, q_z\}$
Unmeasured outputs	$\{\beta, r_x, \dot{r}_x, \dot{q}_z\}$

$\omega_G = (0; 0; 1.30)\ [rad/s]$	RMS	$\boldsymbol{K} = 0$	$\boldsymbol{K}^{\star}$	$\boldsymbol{K}^{\mathrm{LQG}}$	Units
Objective/constraints	$\ddot{\boldsymbol{\beta}}$	0	4.22	4.75	$[rad/s^2]$
$M_y^n = 3.0 \times 10^5$	$\boldsymbol{M}_y$	1.40×10^5	9.11×10^4	1.08×10^5	$[N \cdot m]$
$q_z^n = 2.0 \times 10^{-1}$	$\boldsymbol{q}_z$	6.54×10^{-2}	3.55×10^{-2}	4.55×10^{-2}	$[m]$
$M_x^n = 4.0 \times 10^3$	$\boldsymbol{M}_x$	5.14×10^2	1.13×10^3	8.46×10^3	$[N \cdot m]$
$\beta^n = 1.0 \times 10^{-1}$	$\boldsymbol{\beta}$	0	1.79×10^{-2}	1.04×10^{-2}	$[rad]$
$r_x^n = 5.0 \times 10^{-2}$	$\boldsymbol{r}_x$	2.91×10^{-4}	1.33×10^{-3}	7.14×10^{-3}	$[rad]$
$\dot{r}_x^n = 1.0 \times 10^{-1}$	$\dot{\boldsymbol{r}}_x$	7.91×10^{-3}	4.92×10^{-3}	1.17×10^{-2}	$[rad/s]$
$\dot{q}_z^n = 1.0 \times 10^0$	$\dot{\boldsymbol{q}}_z$	1.42×10^{-1}	1.10×10^{-1}	1.11×10^{-1}	$[m/s]$

Table 2. The RMS norms to three significant figures of the considered outputs in function of the applied control policy for the stationary operating condition $\omega_G = (0; 0; 1.3)\ [rad/s]$.

$\omega_G = (0; 0; 0.95)\ [rad/s]$	RMS	$\boldsymbol{K} = 0$	$\boldsymbol{K}^{\star}$	$\boldsymbol{K}^{\mathrm{LQG}}$	Units
Objective/constraints	$\ddot{\boldsymbol{\beta}}$	0	0.06	0.44	$[rad/s^2]$
$M_y^n = 5.0 \times 10^5$	$\boldsymbol{M}_y$	2.27×10^5	1.57×10^5	3.67×10^5	$[N \cdot m]$
$q_z^n = 2.0 \times 10^{-1}$	$\boldsymbol{q}_z$	9.92×10^{-2}	5.71×10^{-2}	1.25×10^{-1}	$[m]$
$M_x^n = 4.0 \times 10^3$	$\boldsymbol{M}_x$	5.07×10^2	1.22×10^3	2.50×10^3	$[N \cdot m]$
$\beta^n = 1.0 \times 10^{-1}$	$\boldsymbol{\beta}$	0	2.84×10^{-2}	4.90×10^{-2}	$[rad]$
$r_x^n = 5.0 \times 10^{-2}$	$\boldsymbol{r}_x$	2.28×10^{-4}	1.14×10^{-3}	3.06×10^{-3}	$[rad]$
$\dot{r}_x^n = 1.0 \times 10^{-2}$	$\dot{\boldsymbol{r}}_x$	3.43×10^{-3}	3.44×10^{-3}	8.84×10^{-3}	$[rad/s]$
$\dot{q}_z^n = 1.0 \times 10^{-2}$	$\dot{\boldsymbol{q}}_z$	9.11×10^{-2}	9.33×10^{-2}	1.78×10^{-1}	$[m/s]$

Table 3. The RMS norms to three significant figures of the considered outputs in function of the applied control policy for the stationary operating condition $\omega_G = (0; 0; 0.95)\ [rad/s]$.

American Institute of Aeronautics and Astronautics

for an atmospheric turbulence level of $\tau = 6\%$.

The turbine model $\boldsymbol{G}$ is put in closed loop with the optimal control policy $\boldsymbol{K}^\star$ of the reduced system $\boldsymbol{G}_r$ with the objective and additional blade load constraints as discussed in Section III.B for a probability level $\epsilon = 10\%$. For the sake of comparison, a naively tuned LQG controller $\boldsymbol{K}^{\mathrm{LQG}}$ will be considered. The controller $\boldsymbol{K}^{\mathrm{LQG}}$ minimises the proxy cost function

$$J_{\mathrm{LQG}} := \overline{\lim}_{k \to \infty} \quad \sup_{\mathbb{P} \in \mathcal{P}} \mathbb{E}_{\mathbb{P}} \left\{ \gamma \ddot{\boldsymbol{\beta}}^2(k) + \frac{\boldsymbol{M}_y^2(k)}{(M_y^n)^2} + \frac{\boldsymbol{q}_z^2(k)}{(q_z^n)^2} + \frac{\boldsymbol{M}_x^2(k)}{(M_x^n)^2} + \frac{\boldsymbol{\beta}^2(k)}{(\beta_n)^2} + \frac{\boldsymbol{r}_x^2(k)}{(r_x^n)^2} + \frac{\dot{\boldsymbol{r}}_x^2(k)}{(\dot{r}_x^n)^2} + \frac{\dot{\boldsymbol{q}}_z^2(k)}{(\dot{q}_z^n)^2} \right\}$$

for the reduced turbine model $\boldsymbol{G}_r$ where γ is tuned such that the cost of $\boldsymbol{K}^{\mathrm{LQG}}$, as measured by J, is comparable to the cost of the distributionally robust control policy $\boldsymbol{K}^\star$. We remark here that $\boldsymbol{K}^{\mathrm{LQG}}$ is closely related to the control policies reported in [4, 11, 12]. The performance analysis reported in Table 2 indicates that for the same actuation power consumption, the controller $\boldsymbol{K}^{\mathrm{LQG}}$ yields significantly less blade load reduction. We have indicated in grey the quantities for which the corresponding constraints discussed in Section III.B are active, e.g. these quantities are smaller then there nominal values exactly $1 - \epsilon = 90\%$ of the time. We note here that the results reported in Table 2 extend to different atmospheric turbulence levels τ by merit of the linearity of the model $\boldsymbol{G}$ and control policies $\boldsymbol{K}^{\mathrm{LQG}}$ and $\boldsymbol{K}^\star$. To be more specific, the relative difference between the blade load measures reported in Table 2 on our distributionally robust control policy and the standard LQG controller is independent of the atmospheric turbulence level τ. To show that the reported results do not depend dramatically on the operating condition around which $\boldsymbol{G}$ is a valid linearisation of the full nonlinear model derived in Section II, we give the corresponding results for the alternative below rated condition $\nu_0 = (v_G, \omega_G)$ with $v_G = (0; 0; 0)$ $[m/s]$ and $\omega_G = (0; 0; 0.95)$ $[\mathrm{rad}/s]$ in Table 3. It can again be seen that the results obtained using our proposed controller $K^\star$ are superior to a naively tuned LQG controller. Indeed, the LQG controller $\boldsymbol{K}^{\mathrm{LQG}}$ does not meet our design constraints despite using more control actuation than the proposed optimal controller $K^\star$.

V. Conclusion

We proposed an optimal control methodology for the design of gust load controllers for large wind turbine blades. This *distributionally robust* synthesis approach [10] minimises the actuation power expenditure, while guaranteeing that all considered blade load indicators remain bounded in a robust probabilistic sense. Moreover, we indicated that the assumptions made on the turbulence by this methodology are closely related to Kolmogorov's pioneering analysis of flow at high Reynolds numbers [29].

The control approach was tested on a standard 5-MW reference wind turbine [16] and our obtained numerical results indicate that considerable blade load reductions can be achieved as compared to standard LQG control methods. Furthermore, our new proposed method required far less tuning then the LQG synthesis approach as it incorporates the proposed control design objectives and constraints in a straightforward fashion.

Acknowledgements

References

[1] Barlas, T. K. and van Kuik, G., "Review of state of the art in smart rotor control research for wind turbines," *Progress in Aerospace Sciences*, Vol. 46, No. 1, 2010, pp. 27.

[2] Hansen, M.O.L., Srensen, J., Voutsinas, S., Srensen, N., and Madsen, H., "State of the art in wind turbine aerodynamics and aeroelasticity," *Progress in Aerospace Sciences*, Vol. 42, 2006, pp. 285–330.

[3] Bossanyi, E. A., "Individual Blade Pitch Control for Load Reduction," *Wind Energy*, Vol. 6, 2003, pp. 119–128.

[4] Frederick, M., Kerrigan, E., and Graham, J., "Gust alleviation using rapidly deployed trailing-edge flaps," *Journal of Wind Engineering and Industrial Aerodynamics*, Vol. 98, No. 12, 2010, pp. 712–723.

[5]Riziotis, V. A. and Voutsinas, S., "Aero-elastic modelling of the active flap concept for load control," *Proceedings of the EWEC*, Brussels, Belgium, 2008.

[6]Basualdo, S., "Load alleviation on wind turbine blades using variable airfoil geometry," *Wind Engineering*, Vol. 29, 2005, pp. 169–180.

[7]Barlas, T. K. and van Kuik, G., "Aeroelastic modelling and comparison of advanced active flap control concepts for load reduction on the UPWIND 5MW wind turbine," *Proceedings of the EWEC*, Marseille, France, 2009.

[8]Barlas, T. K., van der Veen, G. J., and van Kuik, G., "Model predictive control for wind turbines with distributed active flaps: incorporating inflow signals and actuator constraints," *Wind Energy*, Vol. 15, 2012, pp. 757–771.

[9]Wilson, D., Resor, B. R., Berg, D. E., Barlas, T., and van Kuik, G., "Active Aerodynamic Blade Distributed Flap Control Design Procedure for Load Reduction on the UPWIND 5MW Wind Turbine," *Proceedings of the 48th AIAA Aerospace Sciences Meeting*, Orlando, FL, USA, 2010.

[10]Van Parys, B., Kuhn, D., Goulart, P., and Morari, M., "Distributionally robust control of stochastic dynamical systems," *Optimisation Online*, 2013.

[11]Ng, B., Palacios, R., Graham, J., and Kerrigan, E., "Robust control synthesis for gust load alleviation from large aeroelastic models with relaxation of spatial discretisation," *EWEA 2012, Copenhagen, Denmark*, 2012.

[12]Wilson, D., Berg, D. E., Resor, B. R., Barone, M., and Berg, J., "Combined Individual Pitch Control and Active Aerodynamic Load Controller Investigation for the 5MW UpWind Turbine," *Proceedings of the AWEA Windpower*, Chicago, IL, USA, 2009.

[13]Castaignet, D., Barlas, T., Buhl, T., Poulsen, N. K., Wedel-Heinen, J.J., O. N. A., Bak, C., and Kim, T., "Full-scale test of trailing edge flaps on a Vestas V27 wind turbine: active load reduction and system identificationn," *Wind Energy*, 2013.

[14]Hansen, M. H., "Aeroelastic instability problems for wind turbines," *Wind Energy*, Vol. 10, 2007, pp. 551577.

[15]Bir, G. S. and Jonkman, J., "Aeroelastic Instabilities of Large Offshore and Onshore Wind Turbines," Tech. rep., NREL/CP-500-41804, 2007.

[16]Jonkman, J., Butterfield, S., Musial, W., and Scott, G., "Definition of a 5-MW wind turbine for offshore system development," Tech. rep., NREL/TP-500-38060, 2009.

[17]Hesse, H. and Palacios, R., "Consistent structural linearisation in flexible-body dynamics with large rigid-body motion," *Computers & Structures*, Vol. 110-111, 2012, pp. 1–14.

[18]Palacios, R., Murua, J., and Cook, R., "Structural and aerodynamic models in the nonlinear flight dynamics of very flexible aircraft," *AIAA Journal*, Vol. 48, 2010, pp. 2559–2648.

[19]Murua, J., Palacios, R., and Graham, J., "Applications of the Unsteady Vortex-Lattice Method in Aircraft Aeroelasticity and Flight Dynamics," *Progress in Aerospace Sciences*, 2012.

[20]Murua, J., Palacios, R., and Graham, J., "Assessment of wake-tail interference effects on the dynamics of flexible aircraft," *AIAA Journal*, Vol. 50, 2012, pp. 1575–1585.

[21]Ng, B. F., Hesse, H., Palacios, R., Graham, J.M.R., and Kerrigan, E. C., "Aeroservoelastic Modeling and Load Alleviation of Very Large Wind Turbine Blades," *AWEA Windpower*, Chicago, IL, 2013.

[22]Palacios, R. and Cesnik, C., "Cross-sectional analysis of non-homogeneous anisotropic active slender structures." *AIAA Journal*, Vol. 43, No. 12, 2005.

[23]Simo, J. and Vu-Quoc, L., "On the dynamics in space of rods undergoing large motions - A geometrically exact approach." *Computer Methods in Applied Mechanics and Engineering*, Vol. 66, No. 2, 1988, pp. 125–161.

[24]Géradin, M. and Cardona, A., *Flexible Multibody Dynamics: a Finite Element Approach*, John Wiley, 2001.

[25]Géradin, M. and Rixen, D., *Mechanical Vibrations : Theory and Application to Structural Dynamics*, John Wiley, 2nd ed., 1997.

[26]Katz, J. and Plotkin, A., *Low Speed Aerodynamics*, Cambridge aerospace series, Cambridge University Press, Cambridge, UK ; New York, 2nd ed., 2001.

[27]Zhou, K., Doyle, J., and Glover, K., *Robust and Optimal Control*, Vol. 40, Prentice Hall Upper Saddle River, NJ, 1996.

[28]Burton, T., Jenkins, N., Sharpe, D., and Bossanyi, E., *Wind Energy Handbook*, Wiley, 2011.

[29]Kolmogorov, A., "The local structure of turbulence in incompressible viscous fluid for very large Reynolds numbers," *Dokl. Akad. Nauk SSSR*, Vol. 30, 1941, pp. 299–303.

[30]Campbell, C. W., "Monte Carlo Turbulence Simulation Using Rational Approximations to von Kármán Spectra," *AIAA Journal*, Vol. 24, No. 1, 1986.

[31]Papoulis, A., *Probability, Random Variables, and Stochastic Processes*, McGraw-hill New York, 2002.

[32]Kwakernaak, H. and Sivan, R., *Linear Optimal Control Systems*, Vol. 172, Wiley-Interscience New York, 1972.

[33]Boyd, S. and Vandenberghe, L., *Convex Optimization*, Cambridge university press, 2004.

[34]Tütüncü, R., Toh, K., and Todd, M., "Solving semidefinite-quadratic-linear programs using SDPT3," *Mathematical programming*, Vol. 95, No. 2, 2003, pp. 189–217.

[35]Gugercin, S. and Antoulas, A., "A survey of model reduction by balanced truncation and some new results," *International Journal of Control*, Vol. 77, No. 8, 2004, pp. 748–766.